IOP Conf. Series: Materials Science and Engineering **103** (2015) 012017 doi:10.1088/1757-899X/103/1/012017

A parametric design of ceramic faced composite armor subject to air weapon threats

Y N Guo[1] and Q Sun

School of Aeronautics, Northwestern Polytechnical University, Xi'an, China

E-mail: gyn@nwpu.edu.cn

Abstract. By taking into consideration the two categories of military projectile threats to aircraft structures, an optimal layer configuration of ceramic faced composite armor was designed in this paper. Using numerical simulations and the same layer arrangement of ceramic, UHMWPE, and carbon fiber laminates, a parametric finite element model using LS-DYNA code was built. Several thickness combinations were analyzed in order to determine the final lightest configuration that is capable of supporting a high-speed impact load and HEI blast wave load, which implements a high anti-penetration design for aircraft armor. This configuration can be used to improve the anti-impact ability of aircraft structures as well as achieve a structure/function integration design that considers a lighter weight.

1. Introduction

Air weapons are playing an increasingly important role in modern warfare. However, as ground air defense forces continue to develop, many countries are becoming increasing concerned with the improvement of military aircraft survivability when subjected to ground fire. To ensure safety during flights, structural integrity should be maintained, and the main airframe should have sufficient impact resistance. Lightweight armor systems can efficiently improve the maneuverability, attack ability, and survivability of aircrafts, and they have become a trend for bulletproof armor systems.

For evaluating aircraft structure degradation resulting from a projectile impact, military projectiles of concern in aircraft design can be loosely cataloged into two generic types [1]: (a) non-exploding projectiles and (b) exploding projectiles. For the non-exploding type, typical encounter condition criteria for a low-speed aircraft might be a normal impact at a velocity of 2000ft/s. However, for HEI (High Explosive Incendiary) projectiles, the aircraft damage is a combined effect of fragment impacts and blast pressures. Under fire from HEI, the aircraft should be able to survive the impact and return safely to base.

The armor structure that equips aircrafts needs to possess a good anti-impact performance as well as be able to meet certain special requests, such as aerodynamics and load transfer. Additionally, it must also satisfy weight constraints. Since the 1960s, in which it was first demonstrated that multi-layered armors present advanced strength efficiency when subjected to a high velocity impact, extensive progress has been made in this field. For instance, Wilkins [2] studied the ballistic performance of ceramic tiles backed by aluminum plates against a 7.62 mm projectile. The impact response of ceramic-composite hybrid armor was studied by Woodward using a one-dimensional

[1] Address for correspondence: Y N Guo, School of Aeronautics, Northwestern Polytechnical University, Xi'an, China. E-mail: gyn@nwpu.edu.cn.

approach [3]. Additionally, Wang and others optimized multi-layered armors in order to generate the best performance [4-6]. To improve the ballistic performance, a UHMWPE layer was incorporated with the traditional ceramic armor backed by fiber reinforcement composites, so a three layer configuration was designed in which a ceramic layer works as an energy absorption and dissipation layer, a carbon fiber layer works as a support layer and also a load transfer layer, and a UHMWPE layer works as a flexible layer to absorb the residual energy of the projectile. This configuration can effectively improve the anti-impact ability as well as achieve a structure/function integration design that considers a lesser weight.

In order to improve the anti-impact ability of aircraft structures, research into the anti-impact behaviors of composite armors subject to high-speed impact loads and blast wave loads is implemented based on the theory of impact dynamics and numerical simulation. Through kinematics analysis and ballistic characteristics analysis, an optimal layer configuration is obtained for better ballistic performance.

2. Numerical model

A parametric finite element model was built by using the finite element program LS-DYNA^{TM} [7]. Three layer models were meshed separately and then assembled with an index file. Using the parametric tool built into LS-DYNA, the thickness of every layer could be defined, and the contact relationship could be changed accordingly when the index file calls every layer model as subroutines.

2.1. Index file

The information contained in the index file includes the following:

- Solver control options, such as solve termination time, time step control, and contact parameter options;
- Material mechanical properties of every layer and projectile;
- Contact definitions between the different layers and projectile;
- Initial velocity of the projectile. According to reference 1, vi= 609.6m/s(2000ft/s);
- Amplify factor definitions of every layer using keyword * define transform and simultaneously the location of every layer;
- Call FEA sub-model of every layer using keyword * include transform.

2.2. Sub-model

The index file defined nearly every detail, except for the model geometry information. In the sub-model, the node coordinates and element constructions were built to describe the geometric information of every layer.

The first layer, the ceramic layer, was meshed using solid elements. The central zone mesh was refined to achieve accuracy and to avoid negative volume during impact analysis. The second layer, the carbon fiber layer, was meshed using shell elements, and each element was created by mapping the above ceramic layer. The layup information, such as the thickness and angle of every lamina, was defined by applying the keyword * INTEGRATION_SHELL. Finally, the third layer, the UHMWPE layer, was also built with solid elements.

The projectile (weight of 46 g) was modeled by solid elements with a diameter of 12.7 mm and length of 64.5 mm.

The finite element models of each layer and the projectile are shown in figure 1.

The final complete finite element model is given in figure 1(d), and it indicates the three composite armor layers (ceramic 6 mm, carbon fiber 3 mm, and UHMWPE 5 mm) and the projectile.

2.3. Material model

For the ceramic, carbon fiber, and UHMWPE, three constitutive model were respectively utilized: Johnson Holmquist Ceramics, Enhanced Composite Damage, and User Defined Material Models. Additionally, the Johnson Cook constitutive model was used for the steel projectile. Each material's

mechanical properties are detailed in table 1.

Table 1. Mechanical properties of materials.

Steel(Johnson Cook Model) [8]					
ρ (Kg/m^3)	G(Gpa)	K_1(Gpa)	K_2(Gpa)	K_3(Gpa)	Tm(℃)
7800	78	164	294	500	1520
Cp(J/Kg℃)	A(Gpa)	B(Gpa)	N	C	M
477	0.792	0.510	0.26	0.014	1.03
SiC(Johnson Holmquist Ceramics Model) [9]					
ρ (Kg/m^3)	G(Gpa)	A	B	C	M
3163	183	0.96	0.35	0.0	1.0
N	EPSI	T(Gpa)	SFMAX	HEL(Gpa)	PHEL(Gpa)
0.65	1.0	0.37	0.8	14.567	5.9
D1	D2	K1	K2	K3	BETA
0.48	0.48	204.785	0	0	1.0
CCF-1/5228 Carbon Fiber (Enhanced Composite Damage Model)					
ρ (Kg/m^3)	E_1^{0t} (Gpa)	E_2^0 (Gpa)	G_{12}^0 (Gpa)	G_{23}^0 (Gpa)	ν_{12}^0
1700	146	8.53	4.22	9	0.3
Y_C	Y_0	Y_C'	Y_0'	Y_S'	Y_R
4.29	1.0	1.294	1.0	5.0	1.0
$d_{\max}$	ε_i^{ft}	ε_u^{ft}	d_u^{ft}	E^{0C}	
0.97	0.001	0.005	0.97	23.4	
UHMWPE (User Defined Material Models Hybrid model) [10, 11]					
E(Gpa)	ν	μ_A (Gpa)	λ_A^{lock}	s_{Bi}	s_{Bf}
2.452	0.46	0.00921	2.83	40.0	10.0
α_B	τ_B^{base} (Gpa)	m_B	$\hat{p}$	τ_p^{base} (Gpa)	m_p (Gpa)
27.0	0.0246	9.50	200	0.008	0.0033

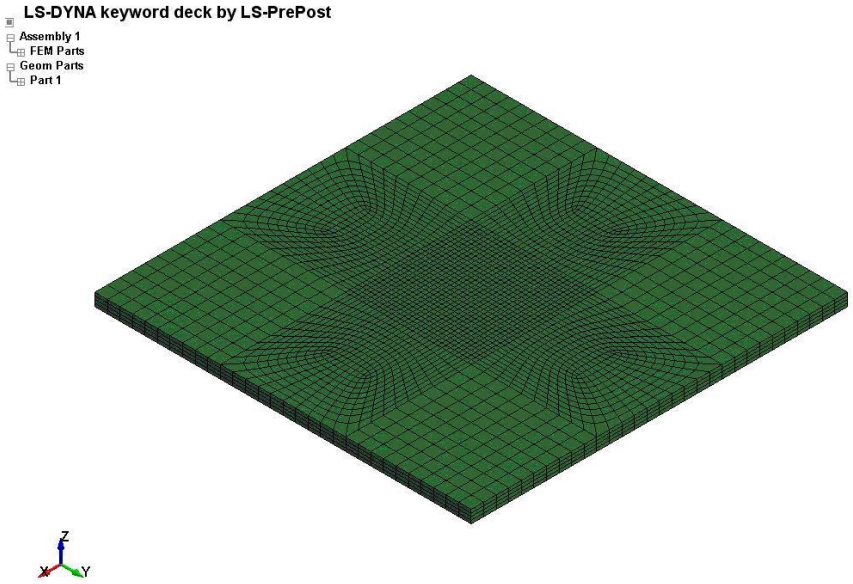

(a)

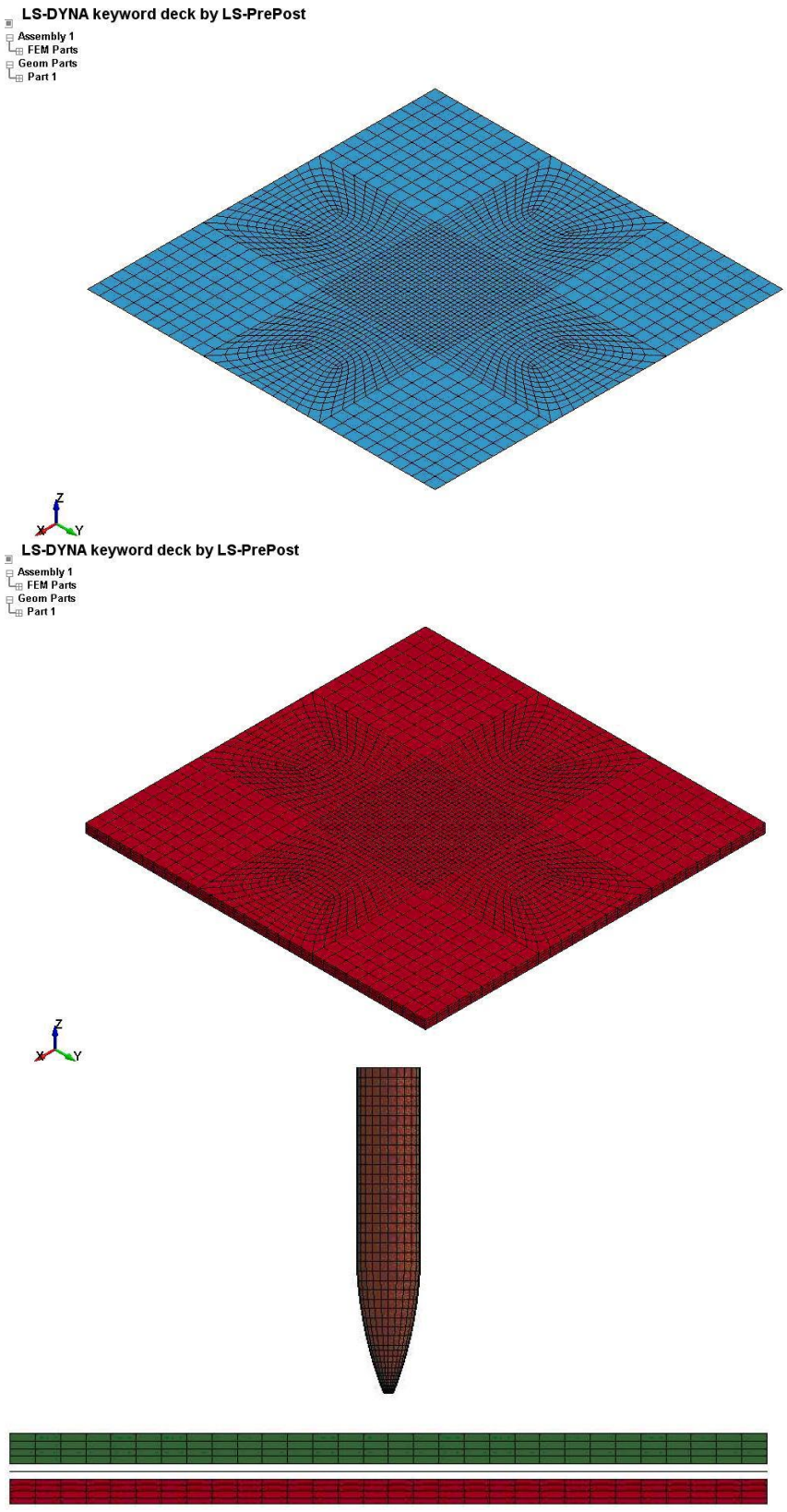

Figure 1. Finite element model. (a) Ceramic layer; (b) Carbon Fiber Layer; (c) UHMWPE Layer; (d) projectile.

3. Selective preference design for high anti-penetration armor

In designing aircrafts, the optimization method is usually the optimal means of achieving a structure that performs well but is also relatively light weight. However, armor impact analysis is very time-consuming, and the process includes some indispensable manual intervention to solve certain issues, such as negative volume, abnormal penetration, and hourglass control. Thus, it is difficult to automatically obtain the best thickness combination for different layers by using the optimization method.

A selective preference design was used, which employed the parametric model so as to intentionally change the amplification factor of every layer. After analyzing every thickness combination, the areal density and the residual kinetic energy are evaluated in order to determine the best armor construction.

Under the initial speed of 609.7 m/s (initial kinetic energy 8.55 KJ), 25 combinations of armor construction were analyzed, and the results are shown in table 2.

Table 2. Armor impact results of various thickness combination.

Armor Arrangement (mm)			Total thickness (mm)	Areal density (g/cm^2)	Residual speed (m/s)	Residual kinetic energy (KJ)	Impact results
SiC	Carbon fiber	UHMWPE					
9.24	0	0	9.24	29.20	-90.3	0.187544	rebound
3	1	11.9	15.9	22.12	413.4	3.93069	penetration
3.5	1	10.2	14.7	22.12	391.2	3.519861	penetration
4	1	8.4	13.4	22.12	388.15	3.46519	penetration
4.5	1	6.8	12.3	22.12	441.3	4.479151	penetration
5	1	5.1	11.1	22.12	436.25	4.377223	penetration
5.5	1	3.4	9.9	22.12	438.9	4.430564	penetration
6	1	1.7	8.7	22.12	439.35	4.439654	penetration
3	2	10.2	15.2	22.12	441.6	4.485243	penetration
3.5	2	8.50	14.00	22.12	430.2	4.256657	penetration
4	2	6.83	12.83	22.12	427.4	4.201427	penetration
5	2	3.44	10.44	22.12	467.0	5.016047	penetration
5.5	2	1.75	9.25	22.12	478.8	5.272737	penetration
6	2.5	4	10.25	26.60	137.9	0.437377	penetration
6.5	2.5	4.28	13.28	28.44	16.4	0.006186	penetration
7	2.5	2.58	12.08	28.44	32.3	0.023996	penetration
3	3	8.52	14.52	22.12	442.1	4.495405	penetration
3.5	3	6.83	13.33	22.12	427.4	4.201427	penetration
4	3	5.13	12.13	22.12	415.2	3.964994	penetration
4.5	3	3.44	10.94	22.12	402.9	3.733553	penetration
5	3	5	13	25.16	49.1	0.055449	penetration
6	3	3	12	26.45	-11.7	0.003148	inlay
3	4	6.84	14.84	22.12	427.3	4.199462	penetration
3.5	4	5.15	12.65	22.12	392.5	3.543294	penetration

From table 2, it can be seen that all the combinations with an areal density of 22.12 were penetrated. With increased total thickness and areal density, two armor constructions were capable of meeting the non-exploding projectile impact design request: the ceramic 6 mm/carbon fiber 3 mm/UHMWPE 3 mm and the single layer ceramic. However, the hybrid construction has a lower areal density than the does the single layer ceramic. The residual velocity of the bullet is 11.7 m/s in the negative direction, which denotes that most of the kinetic energy was absorbed by the armor. The deformation of every layer and the projectile of the preference construction are given in figure 2, and the speed-time curve

of the projectile is shown in figure 3.

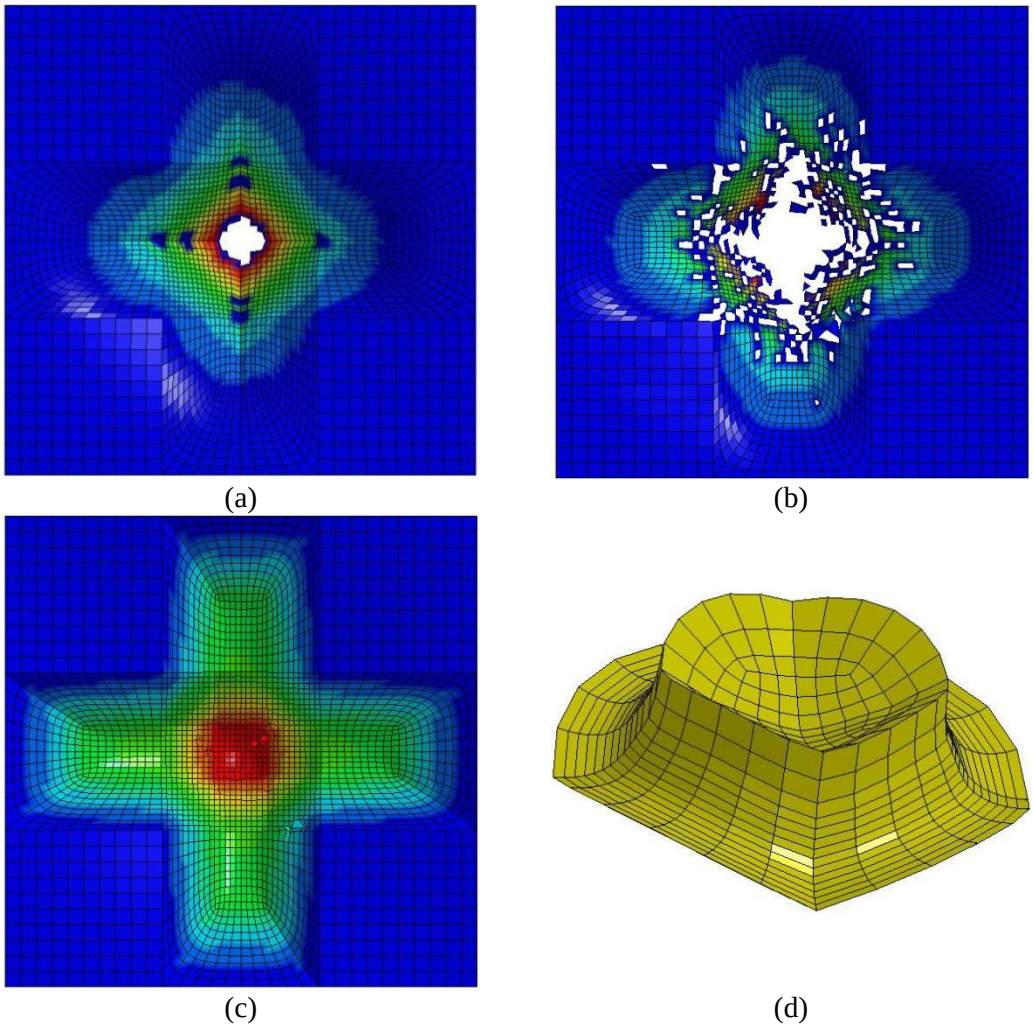

Figure 2. The deformation of every layer and projectile. (a) Deformation of ceramic layer; (b) Deformation of carbon fiber layer; (c) Deformation of UHMWPE layer; (d) Deformation of projectile.

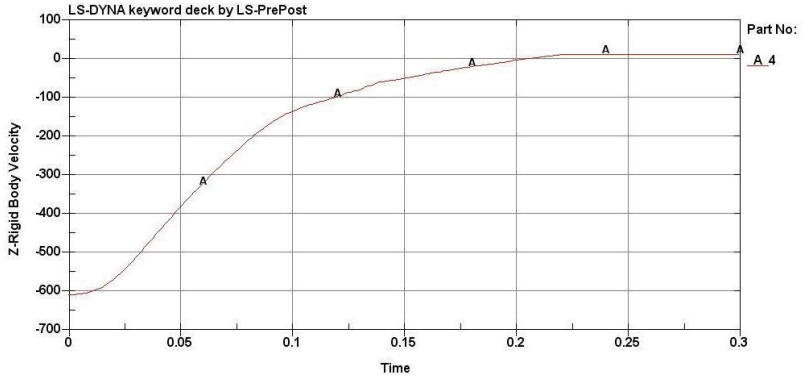

Figure 3. The speed-time curve of the projectile.

4. HEI blast wave load simulation

The armor's response when subjected to another threat, the HEI blast wave load, was analyzed based

on the CJ theory of the blast wave. According to the construction built in reference [12], a finite element model was built to simulate the HEI projectile, as is shown in figure 4. The model contains four parts including the explosive, shell case, infilling, and fragments. For 23 mm HEI, 13.28 g of RDX was used as the ammunition, and the explosive process was calculated with the JWL equation of state. The EOS parameters for RDX are described in table 3.

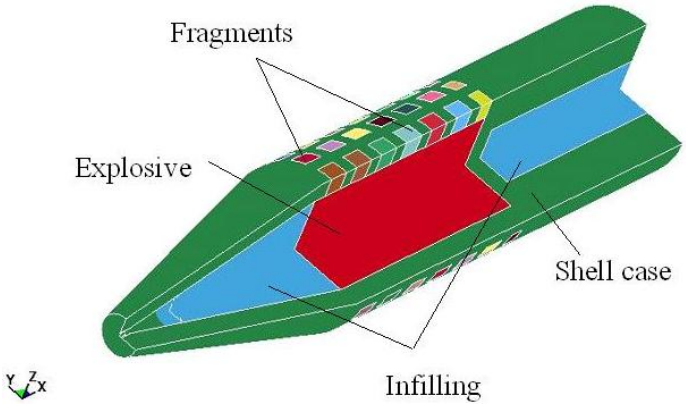

Figure 4. HEI projectile model.

Table 3. RDX explosive parameters.

	component	γ	Density ρ $(g/cm)^2$	Explosive speed (m/s)	Chemical energy release (cal/g)
RDX	(CH2NNO2)3	2.70	1.65	8180	1280

Inside of the HEI projectile, a cylindrical charge (34 mm long and 17 mm in diameter) was meshed. The two-part infillings were used to simulate other concentrated masses other than the explosive, and the total weight of the infillings could be adjusted by changing the density. On the surface of the shell case, 112 rigid parts were distributed so as to simulate the fragments created during an explosion. The mass of each fragment was calculated based on the detonation parameters and the shell case dimensions detailed in reference [12]. The finite element model for each part is shown in figure 5.

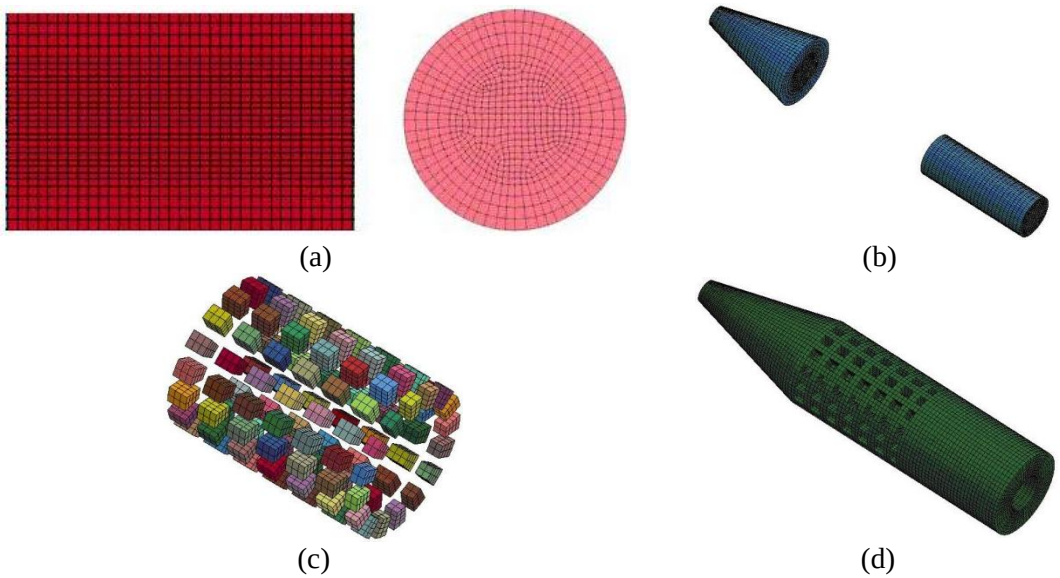

Figure 5. HEI Projectile constructions. (a) RDX explosive; (b) Infillings; (c) Fragments; (d) Shell case.

Following impact with an HEI, the armor experiences a double effect resulting from both the blast wave and the fragment impact. The projectile case would be destroyed because it reached the damage criteria after the explosion. In addition, the rigid fragments flew off at approximately 1500 m/s. The HEI explosion is shown in figure 6, and the speed of some of the fragments are given in figure 7.

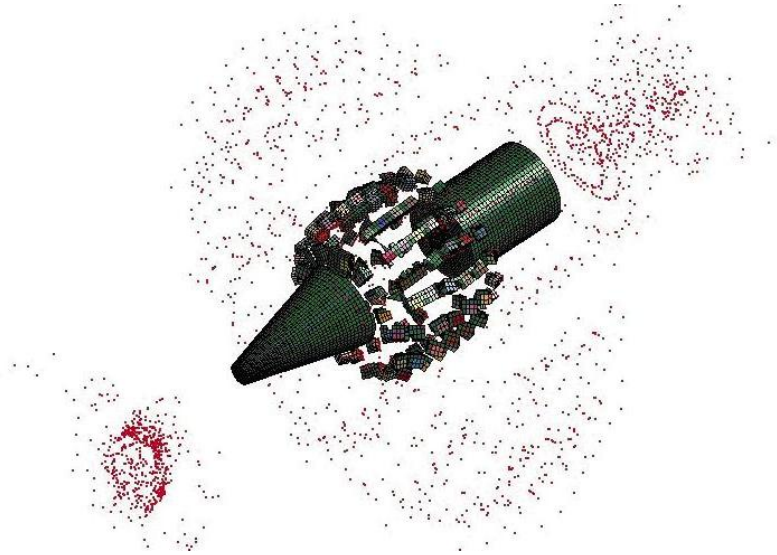

Figure 6. The explosive of HEI (0.012ms).

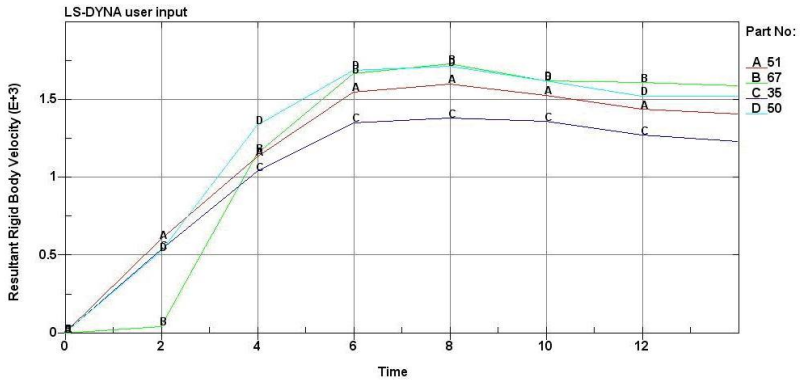

Figure 7. Speed of some fragments.

To test the construction (ceramic 6 mm/carbon fiber 3 mm/UHMWPE 3 mm) obtained in the previous section, an impact response analysis was implemented. The distance between the HEI projectile and the armor was 100 mm. The normal deformation and the maximum stress of the different layers are shown in figure 8.

Figure 8(a) provides a visual representation of the entire impact process. It can be seen that the load takes effect in 0.028 ms, and due to the high speed of the fragment as well as its short distance, no peak deformation appears due to the blast wave until the fragment impacts the armor. At 0.126 ms, under the coupling effect of the blast wave and the fragment, the UHMWPE layer has the first peak displacement, which is 0.286 mm. Then, all three layers return to the equilibrium position due to the recovery elastic force and then continue to deform backwards until 0.24 ms, which is when the ceramic layer reaches its negative peak deformation of 0.126 mm.

Figures 8(b)-8(d) give the stress contour of every layer. The data reveals that no stress exceeded the failure criteria. From the stress contour in figure 8(b), it can be seen that the maximum stress appears in the same pattern as the fragment impact, which indicates that the ceramic layer's function is high-velocity impact resistance. Meanwhile, the patterns in figures 8(c) and 8(d) give a relatively

symmetrical distribution, thus indicating that blast wave absorption is the main function of both the carbon fiber layer and UHMWPE layer.

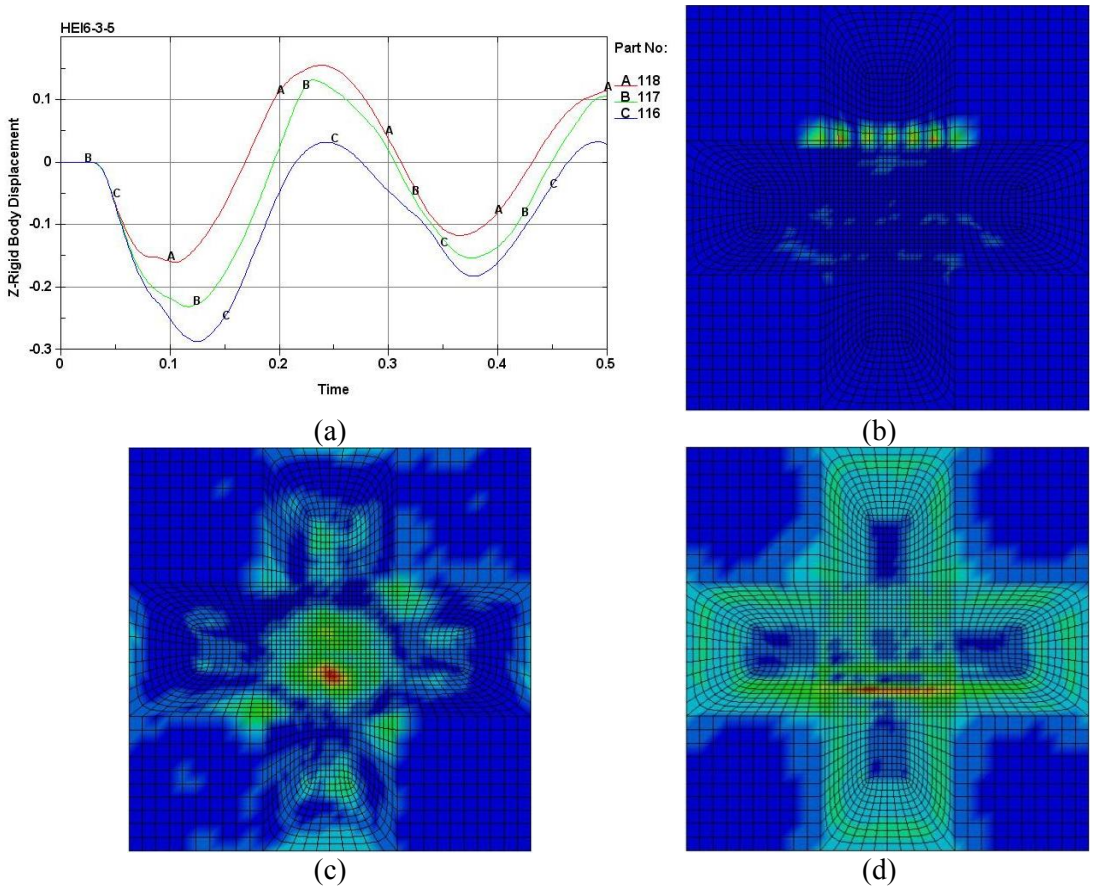

Figure 8. The normal deformation and the maximum stress of different layer. (a) The deformation of each layer(ceramic 118, carbon fiber 117, UHMWPE 116); (b) Maximum stress contour of ceramic layer (maximum stress 6.17 Gpa at 0.09 ms) ; (c) Maximum stress contour of carbon fiber layer(maximum stress 0.672 Gpa at 0.114 ms); (d) Maximum stress contour of UHMWPE layer(maximum stress 0.026 Gpa at 0.092 ms).

5. Conclusions

A parametric finite element analysis was performed in order to obtain an armor arrangement that could meet the criteria for both a non-exploding projectile and an exploding projectile. A 12.7 mm caliber bullet was modeled for a numerical test that evaluated different thickness combinations of composite armor. The best performing armor was attained by a selective preference design, and then, a numerical test with a 23 mm HEI was utilized in order to observe the armor's response to an exploding projectile. The results demonstrated that the armor arrangement is very efficient for both of the two projectile loadings. The armor arrangements and the engineering method could both be important references for improving armor structures.

Acknowledgments

This work is supported by the Fund for basic research from Northwestern Polytechnical University of China (grant no. 0100-GCKY1005).

References

[1] Avery J G 1982 Design manual for impact damage tolerant aircraft structure (AD-A 109290)

[2] Wilkins M L, Landingham R L and Honodel C A 1971 *Fifth Progress Report of Light Armor Program* (Lawrence Radiation Lab. Rept. UCRL-50980)
[3] Woodward R L 1990 A simple one-dimensional approach to modelling ceramic composite armour defeat *Int J Impact Eng*. **9** 455-74
[4] Wang B and Lu G 1996 On the optimisation of two-component plates against ballistic impact *Journal of Materials Processing Technology* **57** 141-5
[5] Park M, Yoo J and Chung D T 2005 An optimization of a multi-layered plate under ballistic impact *International Journal of Solids and Structures* **42** 123-37
[6] Ben-Dor G, Dubinsky A and Elperin T 2005 Optimization of two-component composite armor against ballistic impact *Composite Structures* **69** 89-94
[7] Livermore Software Technology Co. 2007 *ANSYS/LS-dyna Keyword User'S Manual* Vol 1
[8] Johnson G R and Cook W H 983 A constitutive model and data for metals subjected to large strains, high strain rates and high temperatures *Proceedings of the 7th International Symposium on Ballistics* (The Netherlands: Den Haag) vol 1 pp 541-543
[9] Johnson G R and Holmquist T J 1999 Response of boron carbide subjected to large strains, high strain rates, and high pressure *J. Appl. Phys* **85** 8060-73
[10] Bergstrom J S, Rimnac C M and Kurtz S M 2004 An augmented hybrid constitutive model for simulation of unloading and cyclic loading behavior of conventional and highly crosslinked UHMWPE *Biomaterials* **25** 2171-8
[11] Bergstrom J S 2006 Development and implementation of an advanced user material model for UHMWPE *9th International LS-DYNA Users Conference* (Dearborn, MI)
[12] Anderson Jr C E, Sharron T R , Walker J D and Freitas C J 1999 Simulation and analysis of a 23-mm HEI projectile hydrodynamic ram experiment *International Journal of Impact Engineering* **22** 981-97